Geomechanics and Engineering, *Vol. 32, No. 2 (2023) 179-191*
https://doi.org/10.12989/gae.2023.32.2.179

Experimental investigation of earth pressure on retaining wall and ground settlement subjected to tunneling in confined space

Jinyuan Wang[1], Wenjun Li[2], Rui Rui*[1], Yuxin Zhai[3] and Qing He[4]

[1]*School of Civil Engineering and Architecture, Wuhan University of Technology, 122 Luoshi Rd., Wuhan 430070, China*
[2]*China Harbour Engineering Company Ltd., 9 Chunxiu Rd., Dongzhi gate, Dongcheng District, Beijing 100027, China*
[3]*China Railway Construction Group Co., Ltd., No. 69 Fuxing Road, Haidian District, Beijing 100040, China*
[4]*China Fortune Land Development Co., Ltd., No. 18 Xiaguangli, Dongsanhuan North Road, Chaoyang District, Beijing 100027, China*

(*Received September 3, 2021, Revised January 2, 2023, Accepted January 6, 2023*)

Abstract. To study the influences of tunneling on the earth pressure and ground settlement when the tunnel passes through the adjacent underground retaining structure, 30 two-dimensional model tests were carried out taking into account the ratios of tunnel excavation depth (*H*) to lateral width (*w*), excavation width (*B*), and excavation distance using a custom-made test device and an analogical soil. Tunnel crossing adjacent existing retaining structure (TCE) and tunnel crossing adjacent newly-built retaining structure (TCN) were simulated and the earth pressure variations and ground settlement distribution during excavation were analyzed. For TCE condition, the earth pressure increments, maximum ground settlement and the curvature of the ground settlement curve are negatively related to *H*/*B*, but positively related to *H*/*s* and *H*/*w*. For TCN condition, most trends are consistent with TCE except that the earth pressure increments and the curvature of ground settlement curve are negatively related to *H*/*w*. The maximum ground settlement is larger than that observed in tunnel crossing the existing underground structure. This study provides an assessment basis for the design and construction under confined space conditions.

Keywords: analogical soil; earth pressure; ground settlement; model test; retaining wall; tunneling

1. Introduction

With the utilization of subsurface, the conditions for shield tunnel, foundation pit engineering and all kinds of pipelines and pipe gallery intersected and constructed simultaneously happen more and more frequently (Buchatskii *et al.* 2001, Leung and Meguid 2011). The underground excavation inevitably causes the deformation of the surrounding soil and the earth pressure variation of surrounding retaining structures, which may induce the ground settlement and the destruction of surrounding buildings and underground pipelines (Stiros and Kontogianni 2009, Hesami *et al*. 2019).

In the urban subsurface environment, the boundary conditions are always confined by basements, foundation pits or large pile groups (Som and Das 2003). When tunnel passes through the stratum near the retaining wall of the basement or the pile group, it will cause nonlinear changes of the earth pressure and deformation (Yoo *et al.* 2019). Yamaguchi *et al.* (1998) analyzed the influence of shield tunneling on adjacent existing structures from the aspects of design and construction, respectively. Jenck and Dias (2004) adopted finite difference method and 3D finite element method to establish the 3D numerical model for the tunnel excavation and adjacent buildings. The influence of tunneling on adjacent structures was analyzed. Lee (2019) conducted an experimental study on the changes in earth pressure and ground settlement due to underground excavation near an existing retaining wall. The effect of the underground excavation distance on the behaviors of the retaining wall was elaborated and the arching effect exhibited during the subsurface construction was experimentally proved.

For the underground excavation, Peck (1969) found that the ground surface settlement obeys normal distribution and proposed a formula for estimating the distribution of the surface settlement and the maximum settlement through statistical analysis of a large number of ground settlement data. Attewell and Woodman (1982) and Rowe *et al*. (1983) corrected and supplemented the formula. Attewell and Woodman developed the formula for the prediction of the three-dimensional ground settlements and strains caused by tunneling in soil. Rowe et al. identified the possible effects of different parameters (e.g., elastic modulus, angle of friction, the coefficient of lateral earth pressure at rest, and ground loss) upon predicted surface settlement. Ding *et al.* (2017) proposed that surface settlement presented the characteristics of cork distribution curve, skewed distribution curve and normal distribution curve when the tunnel was under buildings, within the scope of the disturbance and outside the scope of the disturbance, respectively. They verified the above surface settlement characteristics through numerical simulation, experimental comparison and model test analysis. Chakeri *et al.* (2013) and Dias and Kastner (2013) discussed the influences of important factors like tunnel depth, tunnel dimension, overburden pressure, face pressure, and the grout injection

*Corresponding author, Professor
E-mail: r.rui@whut.edu.cn

ISSN: 2005-307X (Print), 2092-6219 (Online)

in the annular void on the ground settlement of shield tunnel excavation. However, under the complex urban boundary conditions, such as underground excavation near retaining structures or in lateral confined conditions with narrow space (Hunt *et al.* 2016, Srikar and Mittal 2021), the empirical prediction of ground deformation caused by underground excavation may be quite different from infinite space condition (Lam *et al*. 2014, Kakrasul 2018). Furthermore, for the frequent conditions that tunnel crossing the adjacent existing/newly-built underground retaining structure, to the best of the authors' knowledge, few studies have been reported to specifically examine the regularity of the ground settlement.

In most cases, tunneling will induce ground loss and ground settlement due to stress release (Peck 1969). Tunneling may also cause ground collapse in some extreme cases (Kavvadas 2005, Yum *et al*. 2020). To investigate the earth pressure and ground settlement involved in the tunneling in the confined space conditions, a trapdoor device was developed for the model tests. The trapdoor was used to simulate ground loss of tunneling. For two conditions, which are tunnel passing through adjacent existing retaining structures (TCE) and tunnel passing newly-built retaining structures (TCN), respectively, the earth pressure distribution of underground retaining structures and ground settlement under confined conditions are discussed.

2. Theoretical considerations

2.1 Static earth pressure

Jaky (1944) derived a formula for calculating the static earth pressure, σ_0, without considering wall-soil friction.

$$\sigma_0 = \gamma z\left[(1-\sin\varphi)\frac{1+\frac{2}{3}\sin\varphi}{1+\sin\varphi}\right] \tag{1}$$

where, φ is the internal friction angle of the soil, γ the gravimetric density of the soil mass and z the burial depth of the soil mass.

Janssen (1895) assumed that the shape of the soil arch was horizontal rectangle and established the horizontal differential equation. The formula considering wall-soil friction is called Janssen's static earth pressure $\sigma_{h,J}$.

$$\sigma_{h,J} = \frac{\gamma w}{2\mu}\left[1-\exp\left(-2k_0\mu\frac{z}{w}\right)\right] \tag{2}$$

where, w is the width of the fill, μ the wall-soil friction coefficient that equals the tangent value of the wall-soil friction angle δ.

2.2 Active earth pressure

Rankine (1857) assumed that the back of the wall was vertical and frictionless, and the surface of the backfill was horizontal, and the formula for calculating the active earth pressure σ_a was derived.

$$\sigma_a = \gamma\cdot z\cdot K_a \tag{3}$$

$$K_a = \tan^2\left(45°-\frac{\varphi}{2}\right) \tag{4}$$

where, K_a is the active earth pressure coefficient.

According to the force equilibrium condition of triangular soil wedge, Coulomb (1776) derived the formula for calculating active earth pressure $\sigma_{a,C}$.

$$\sigma_{a,C} = \gamma\cdot z\cdot K_{a,C} \tag{5}$$

$$K_{a,C} = \frac{\cos^2(\varphi-\alpha)}{\cos^2\alpha\cdot\cos(\alpha+\delta)\cdot\left[1+\sqrt{\frac{\sin(\varphi+\delta)\sin(\varphi-\beta)}{\cos(\alpha+\delta)\cos(\alpha-\beta)}}\right]^2} \tag{6}$$

where, $K_{a,C}$ is the Coulomb active earth pressure coefficient, α the angle at which the wall face inclined to the vertical, β the dip angle of the backfill surface.

For semi-infinite space, Handy (1985) considered the deflection effect of the backfill, and derived the theoretical active earth pressure $\sigma_{a,H}$.

$$\sigma_{a,H} = \frac{\gamma(H-z)\tan\left(45°-\frac{\varphi}{2}\right)}{\mu}\cdot\left[1-\exp\left(-K_{a,H}\mu\frac{z}{(H-z)\tan\left(45°-\frac{\varphi}{2}\right)}\right)\right] \tag{7}$$

$$K_{a,H} = 1.06\left(\cos^2\theta + K_{a,k}\sin^2\theta\right) \tag{8}$$

where, $K_{a,H}$ is the Coulomb active earth pressure coefficient, θ the angle of the slip surface which equals (45°+φ/2), H the height of the retaining wall, and z the buried depth.

Based on the assumption that the backfill is a sliding wedge at the limit equilibrium state, Harrop-Williams (1989) derived a general formula which can be used to calculate the active and passive earth pressure (σ_{HW}) for the translation and rotation of the retaining wall.

$$\sigma_{HW} = K_{HW}\gamma H\frac{(1-\frac{z}{H})-(1-\frac{z}{H})^{\beta-1}}{\beta-2} \tag{9}$$

$$K_{HW} = \frac{1+K_a\tan^2\psi_{HW}}{\tan^2\psi_{HW}+K_a} \tag{10}$$

where, β is the deflection coefficient of the backfill, Ψ_{HW} the angle of the slip surface, K_{HW} the Harrop-Williams theoretical earth pressure coefficient.

$$\tan\psi_{HW} = \frac{1-K_a}{2K_a\tan\delta}\pm\left[\left(\frac{1-K_a}{2K_a\tan\delta}\right)^2-\frac{1}{K_a}\right]^{\frac{1}{2}} \tag{11}$$

$$\beta = K_{HW}\frac{\left\{(\cos\delta)^{\frac{1}{2}}\pm\left[\sin(\varphi+\delta)\sin\varphi\right]^{\frac{1}{2}}\right\}^2}{\cos^2\varphi} \tag{12}$$

The positive expressions are applicable to the calculation of active earth pressure, and the negative expressions are applicable to the calculation of passive earth pressure.

Paik and Salgado (2003) derived the formula of theoretical active earth pressure $\sigma_{a,P}$ based on differential element.

$$\sigma_{a,P}=\frac{\gamma H K_{a,P}}{1-K_{a,P}\tan\delta\tan\theta}\left[\left(1-\frac{z}{H}\right)^{K_{a,P}\tan\delta\tan\theta}-\left(1-\frac{z}{H}\right)\right] \tag{13}$$

$$K_{a,P}=\frac{3\left(N\cos^2\psi_P+\sin^2\psi_P\right)}{3N-(N-1)\cos^2\psi_P} \tag{14}$$

$$\psi_P=\tan^{-1}\left[\frac{(N-1)\pm\sqrt{(N-1)^2-4N\tan^2\delta}}{2\tan\delta}\right] \tag{15}$$

where, $K_{a,P}$ is the Paik theoretical active earth pressure coefficient, Ψ_P the principle stress deflection angle of the soil behind the wall, N=1/$K_{a,C}$.

2.3 Surface settlement curve

Peck (1969) assumed that under the undrained condition, the volume of the surface settlement trough caused by underground excavation was equal to the volume of the ground loss, and the ground loss was evenly distributed in the direction of tunnel excavation. He proposed that the transverse surface settlement trough was approximately normal distribution, and provided the prediction formula for the ground settlement.

$$S(x)=\frac{AV_l}{i\sqrt{2\pi}}\cdot\exp\left(-\frac{x^2}{2i^2}\right)\approx\frac{AV_l}{2.5i}\cdot\exp\left(-\frac{x^2}{2i^2}\right) \tag{16}$$

where, $S(x)$ is the settlement of any point on the ground, i the width of the settlement trough representing the distance from the symmetry center of the settlement curve to the inflection point, x the distance from the calculated point to the symmetric center, A the excavation area, V_l the ground loss rate.

The width of the settlement trough i in Eq. (16) can be calculated by Eq. (17).

$$i=\frac{H}{\sqrt{2\pi}\tan\left(\pi/2-\varphi\right)} \tag{17}$$

where, H is the burial depth at the center point of the tunnel.

3. Test setup and test program

3.1 Test setup

The excavation processes such as shield tunneling are very complicated. To investigate variations of the earth pressure on the retaining wall and ground settlement when the tunnel crosses the adjacent existing and newly-built underground retaining wall, a custom-made two-dimensional device was built and simplified geometry and conditions were considered, as shown in Fig. 1. The device is composed of a fill box, an earth retaining plate with a displacement controller, a pressure measurement plate, a trapdoor displacement controller and an outer frame.

The maximum size of the fill box is 800 mm wide and 665 mm high. The pressure measurement plate, which consists of 18 cantilever-beam load gauges, is installed on the earth retaining plate to measure the earth pressure transmitted to the retaining structure. The displacement controller is connected to the back of the earth retaining plate. The displacement of the retaining wall can thus be accurately controlled so as to simulate a translation mode of the retaining wall.

The boundary condition of the model test was simplified to a two-dimensional condition by using the two-dimensional analogical soil. The analogical soil is formed by mixing elliptical steel rods of three sizes (Size A: 3 mm× 6 mm; Size B: 4 mm× 8 mm; and Size C: 5 mm× 10 mm, defined as short axis versus long axis) with a mass ratio of 1:1:1. Each lift of 25 mm thick fill had 594 rods of Size A, 334 rods of Size B, and 214 rods of Size C, which were mixed thoroughly and used to fill the chamber. The length of the steel rods was 300mm. To verify the similarity between the two-dimensional behavior of the analogical soil and the sand fill, biaxial compression tests were carried out.

The stress-strain curves obtained from the tests are similar to those of the dense sand, which well reflects the peak strength and dilatancy of the sand. The peak friction angle φ_p is 34° with a diltancy angle ψ_m of 5° under a confining pressure of 50kPa, and the repose angle of the analogical soil measured by repose angle tests is 28.2°. The steel rods are filled by layers and sufficiently vibrated to make the analogical soil reach the most compact state. The porosity corresponding to this state is about 0.16, and the corresponding bulk density is 65.93 kN/m^3, which is approximately four times that of a typical sand and improves the similarity ratio. This high ratio results in a stress in the fill that is closer to the stress in full-scale situations.

Compared to the real sand, the analogical soil is found to be easily to be compacted and obtain the largest relative density. The relative density of the constructed backfill can be regarded as almost 100%. Because the outer frame, the pressure measurement plate and analogical soil materials are all made of steel, δ and φ are taken as the repose angle of the analogical soil (i.e., 28.2°). The transparent front and back walls were taken off to eliminate the friction from the front and back. Therefore, the backfill consisting of steel rods is simplified to a plane-strain problem and reduced to a two-dimensional condition.

The trapdoor displacement controller is composed of 10 steel movable plates and an elevator. Each movable plate is 75 mm wide, and can be connected to the displacement

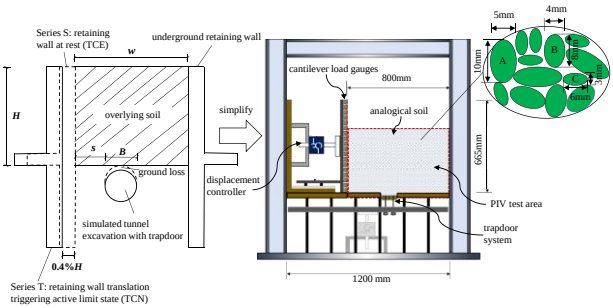

Fig. 1 Simplified schematic diagram of model test

Table 1 Test program

Test ID	H (mm)	w (mm)	B (mm)	s (mm)	H/w	H/B	H/s
S1/T1	600	600	75	225	1	8	2.67
S2/T2	600	600	75	150	1	8	4
S3/T3	600	600	75	75	1	8	8
S4/T4	600	600	150	225	1	4	2.67
S5/T5	600	600	150	150	1	4	4
S6/T6	600	600	150	75	1	4	8
S7/T7	600	600	225	150	1	2.67	4
S8/T8	600	600	225	75	1	2.67	8
S9/T9	600	450	75	150	1.3	8	4
S10/T10	600	450	75	75	1.3	8	8
S11/T11	600	450	150	150	1.3	4	4
S12/T12	600	450	150	75	1.3	4	8
S13/T13	600	450	225	75	1.3	2.67	8
S14/T14	600	300	75	75	2	8	8
S15/T15	600	300	150	75	2	4	8

controller through bolts to simulate the ground loss caused by underground excavation. The ground loss is accurately controlled by the elevator manually using a dial indicator. Particle image velocimetry (PIV) technology (White *et al*. 2003) is used to obtain the displacement.

The ground loss usually refers to the difference between the volume of the actual excavated soil and the volume of the tunnel after the completion of construction. Peck (1969) assumed that the volume of the settlement trough is equal to that of the ground loss. The ground loss rate V_l is defined as

$$V_l = \frac{S_1}{S_2} \tag{18}$$

where, S_1 is the area of ground loss, S_2 the area of tunnel excavation.

Wei (2010) statistically analyzed the data of ground loss in China and found that the ground loss rate ranged from 0.2% to 2.0% for Shield TBM (Tunnel Boring Machine). Assuming that the top of trapdoor is the top point of the circular tunnel, the volume of the trapdoor settlement is equal to the ground loss induced by the tunnel excavation.

The deformation distribution caused by tunnel excavation is not uniform in the transverse plane of the tunnel. Rui *et al*. (2019) found that the non-uniformity of ground loss disappeared above the height of 1.5 times the width of the trapdoor from the top of the trapdoor, and the deformation was only related to the settlement volume beyond the height. Therefore, trapdoor can roughly simulate the tunnel excavation. In this study, the ground loss rate is set to be 0.85%. Accordingly, for the excavation widths B of 75 mm, 150 mm and 225 mm, the movements of the trapdoor are 0.5 mm, 1 mm and 1.5 mm, respectively.

3.2 Test program

The tests consider two conditions. For the condition represented by Series S, the tunnel crosses an adjacent existing retaining structure and the backfill is in a stable and rest state. For the condition labelled T, the tunnel crosses an adjacent newly-built retaining structure, which means that the backfill approaches the active limit equilibrium state.

The two conditions both regard the lateral width (i.e., width of the backfill) w, the excavation distance (from the excavation edge to the back of the retaining wall) s, and the excavation width B, as the test parameters. The lateral widths are 600mm, 450mm and 300 mm, the excavation distances are 225 mm, 150 mm and 75 mm, and the excavation widths are 225 mm, 150mm and 75 mm, respectively. The excavation depth H is set to be 600 mm.

The model test program includes 30 tests as listed in Table 1. Before the tests, the position of the retaining plate is adjusted to obtain the prescribed lateral width, and the steel rods are then filled in layers. After the filling height reaches 600 mm, the load gauge reading is recorded to obtain the lateral earth pressure at rest.

For Series S, after the completion of the filling, the trapdoor is controlled to lower at a movement interval of 0.01 mm to the required movement. Every image of the backfill profile is collected for PIV analyses and the corresponding load gauge data are recorded for each movement interval. After reaching the required settlement for the ground loss rate of 0.85%, keep on lowering the trapdoor until the trapdoor settlement reaches 40 mm.

For Series T, the first step is to control the translation of the retaining plate against the soil (active mode). The image of the backfill profile and the corresponding load gauge data are recorded at the translational displacement interval of 0.01 mm too. When the active displacement reaches 0.4 %H (i.e., 2.4 mm, reaching the active limit state), the translation displacement is terminated. The second step is to lower the trapdoor. Similarly, images and the corresponding load gauge readings are recorded every 0.01 mm movement interval until the settlement of the trapdoor reaches 40 mm.

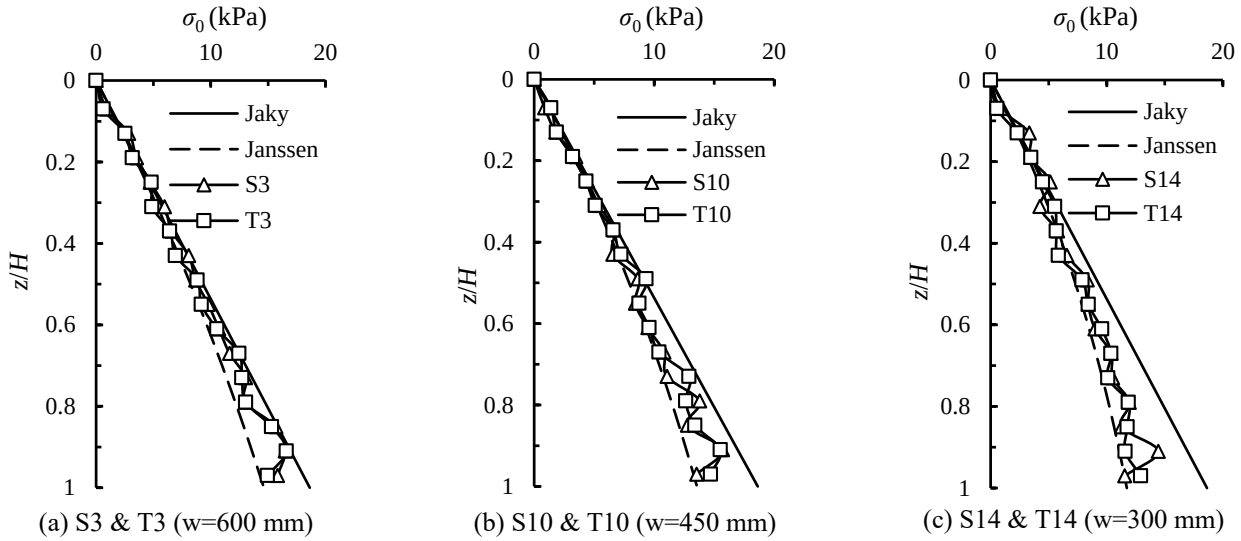

(a) S3 & T3 (w=600 mm) (b) S10 & T10 (w=450 mm) (c) S14 & T14 (w=300 mm)

Fig. 2 Distribution of earth pressure at rest

4. The influence of under-crossing tunneling on the earth pressure of the retaining wall

4.1 Earth pressure at rest

Taking the tests S3, S10, S14 and T3, T10, T14 as example, the earth pressures at rest are plotted against the burial depth z normalized by the excavation depth H as shown in Fig. 2.

Within the burial depth, the earth pressure at rest is basically linearly distributed. With the increase of the burial depth, the earth pressure presents a nonlinear distribution due to the influence of the friction on the walls of the fill box. The smaller the lateral width is, the more significant the friction effect is. The lateral earth pressure for w=300mm has a larger deviation due to the larger friction influence from the narrow boundary.

The measured results are compared with those calculated by the Jaky's method without considering the friction effect and the Janssen's method considering the friction effect from the walls of the fill box. It is found that the measured earth pressure acted on the retaining wall are between the calculation values by the two methods. When the lateral width is small, the measured earth pressure is close to the calculation of Janssen's method considering the friction effect with a friction angle of 28.2°. When the lateral width is large, the measured earth pressure is close to the calculation of the Jaky's method.

4.2 Earth pressure distribution during retaining plate translation

During the translation process of the retaining plate, the backfill gradually transits from the static state to the active limit state. Terzaghi (1934) proposed that the active displacement required for dense sand to reach the active limit state was 0.1%H, while Matsuo *et al.* (1978) and Khosravi *et al.* (2013) found that the active displacement required for the back fill to reach the active limit state was between 0.2% and 0.8% H (0.6 ~ 0.8%H for silty sand in Matsuo et al. and 0.2%H in average for silica sand No.8 in Khosravi *et al*. 2013). For different types of soils and retaining walls, the required displacement to reach the active limit state may be different. For the analogical soil used in this study, the active limit state can be determined by observing the earth pressure distribution during the retaining wall translation.

Fig. 3 shows the distribution curve of the earth pressure p on the retaining plate at the translation displacements of 0.2%H and 0.4%H for tests T3, T10 and T14. The Rankine active earth pressure and Coulomb active earth pressure are calculated and compared with the measured earth pressure.

With the increase of translation displacement, the earth pressure of retaining wall decreases. When the translation displacement reaches 0.2%H, the measured earth pressure is close to Rankine active earth pressure. When the displacement is increased to 0.4%H, the measured earth pressure is close to the Coulomb active earth pressure considering wall-soil friction effect. Therefore, it can be concluded that for the adopted analogical soil, the active displacement required to reach the active limit state is 0.4%H.

It is noted that the measured earth pressure is nonlinear, which consists of a straight part and a curved part at the bottom divided by a turning point. Below the turning point, the decline of earth pressure can be attributed to the "bin effect" (Handy 1985).

For further analysis, the measured earth pressures corresponding to the 0.4%H retaining wall displacement are compared with the calculation results from Handy's method, Harrop-Williams' method and Paik's method considering wall-soil friction and soil-arching effect.

As shown in Fig. 4, Paik's method agrees best with the measured active earth pressure. The maximum earth pressure of Paik's method locates at z/H=0.7, while the maximum values of Handy and Harrop-Williams earth pressures locate near z/H=0.6.

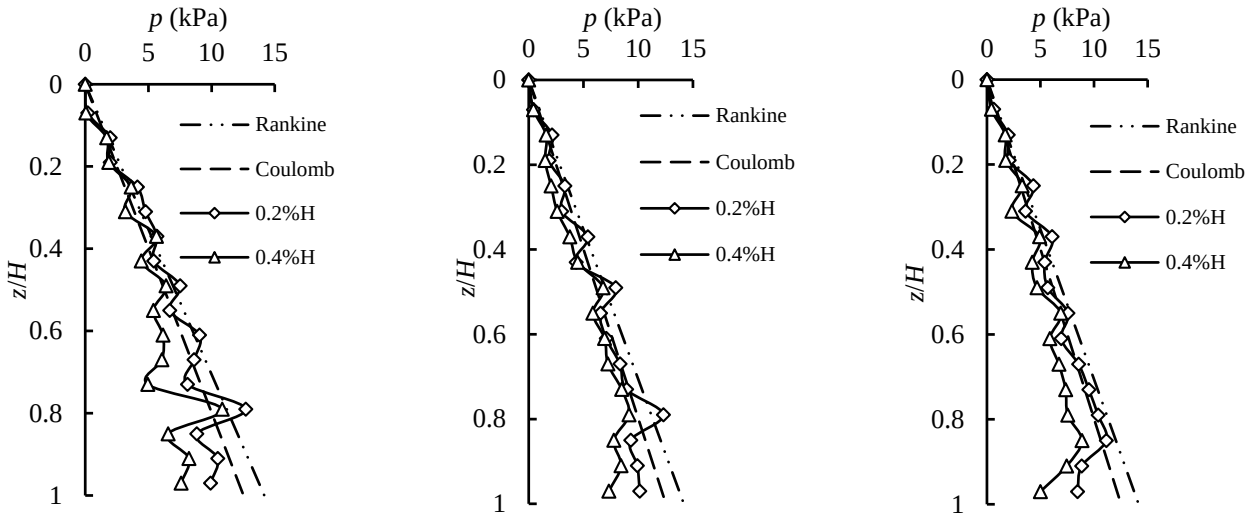

(a) T3 (w=600 mm) (b) T10 (w=450 mm) (c) T14 (w=300 mm)

Fig. 3 Distribution of earth pressure in the process of retaining wall translation

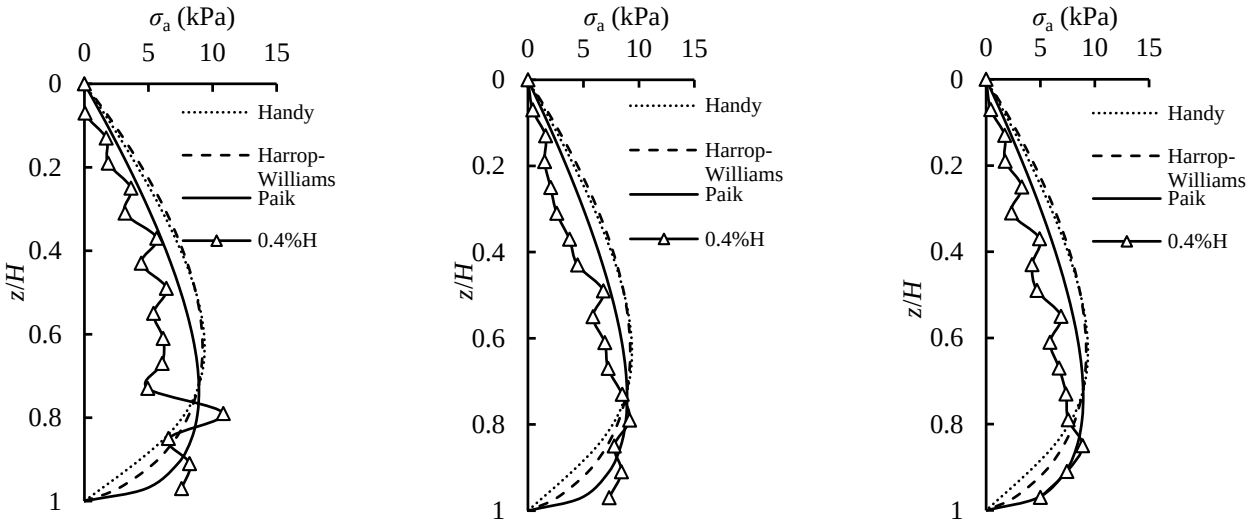

(a) T3 (w=600 mm) (b) T10 (w=450 mm) (c) T14 (w=300 mm)

Fig. 4 Distribution of active earth pressure

4.3 The influence of the tunnel excavation process

To study the variation of the earth pressure on the existing/newly-built underground retaining structures during the tunnel excavation, Fig. 5 compares the earth pressure increments (the subtraction of measured earth pressure and the earth pressure at rest or after 0.4%H retaining wall displacement) Δp of test S3 (TCE) and T3 (TCN).

As shown in Fig. 5(a), the earth pressure at the bottom of the retaining wall decreases with the settlement of the trapdoor, while the earth pressure increment curve has a turning point at about z/H= 0.8. The earth pressure above the turning point increases. The absolute values of the earth pressure increments below and above the turning point both increase with the settlement of the trapdoor. Meanwhile, the turning point gradually elevates with the trapdoor settlement. The variation of the earth pressure tends to be.

In contrast, with the trapdoor settlement in test T3, the earth pressure increments of newly-built retaining wall, which means the soil is disturbed by the displacement of the retaining wall, increases in the whole range of burial depth, as observed in Fig. 5(b). The earth pressure increments on the bottom of the retaining wall is the largest along the entire burial depth. Deferent from test S3, the earth pressure increments keep on increasing with the settlement.

4.4 The influence of the ratio of tunnel excavation depth to excavation width

Tests 2, 5 and 7 with the same lateral width w and excavation distance s (w=600 mm, s=150 mm) form a test group with various ratios of excavation depth to excavation width (H/B=8, 4, 2.7). The test groups corresponding to the

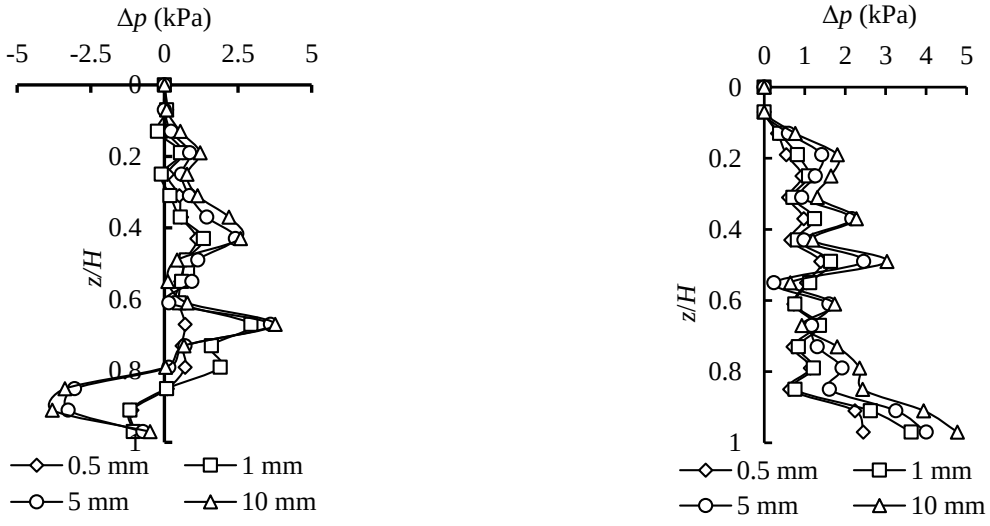

(a) S3 (b) T3

Fig. 5 Distribution of earth pressure increments during trapdoor settlement

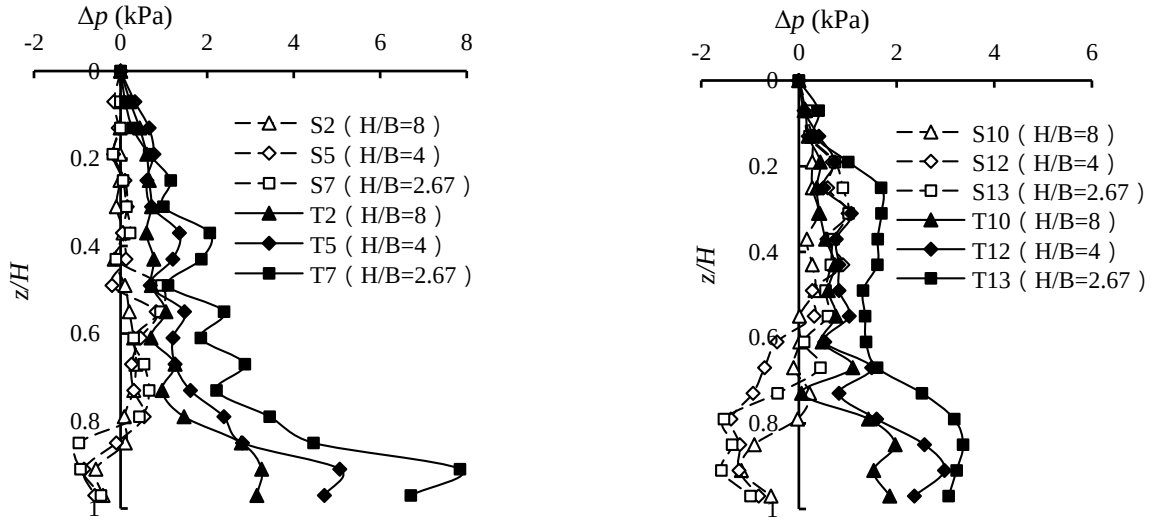

(a) w=600 mm, s=150 mm (b) w=450 mm, s=75 mm

Fig. 6 Distribution of earth pressure increments under different *H*/*B*

two conditions (TCE and TCN) are selected to study the influence of *H*/*B*. As aforementioned, for the excavation widths *B* of 75 mm, 150 mm and 225 mm, the settlements of the trapdoor Δ are 0.5 mm, 1 mm and 1.5 mm, respectively.

The relationship between the earth pressure increments of the retaining wall Δp and the normalized burial depth *z*/*H* for the test groups is shown in Fig. 6.

When the tunnel crosses an existing underground retaining structure (Series S in Fig. 6), for the same ground loss rate with the same *H* of 600 mm, the smaller the *H*/*B* is, the greater the absolute value of *B* and the ground loss are. Thus the unloading is more significant. As a consequence, the earth pressure at the bottom of the retaining wall decreases, while the earth pressure above the turning point increases, which could be attributed to the arching effect supported by the wall friction from the bottom and the retaining plate above the turning point. The turning point of the earth pressure distribution elevates accordingly with the decrease of *H*/*B*.

For Series T in Fig. 6, no turning point of earth pressure distribution appears when the tunnel crosses the newly-built underground retaining structure. Due to the disturbed backfill, the earth pressure on the retaining structure increases a lot, especially on the lower part. Under the same ground loss rate, the smaller the *H*/*B* is, the greater the earth pressure increments are.

4.5 The influence of the ratio of tunnel excavation depth to excavation distance

To study the variation of the earth pressure on the retaining structure when tunnel crosses existing and newly-built underground retaining structures, ratios of tunnel

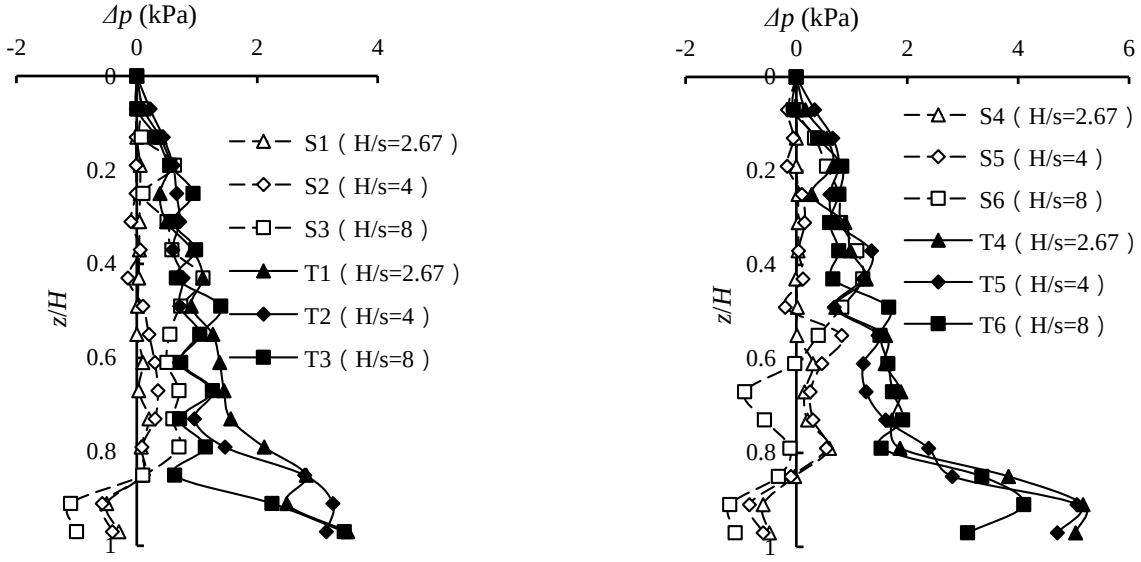

(a) w=600 mm, B=75 mm (Δ=0.5 mm) (b) w=600 mm, B=150 mm(Δ=1 mm)

Fig. 7 Distribution of earth pressure increments under different H/s

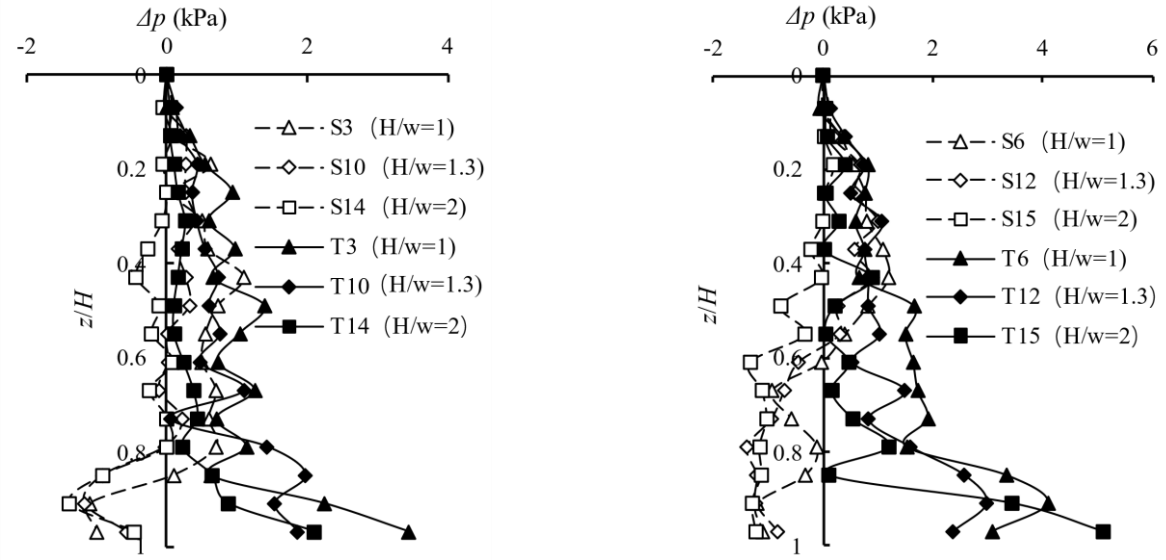

(a) s=75 mm, B=75 mm (Δ=0.5 mm) (b) w=75 mm, B=150 mm (Δ=1 mm)

Fig. 8 Distribution of earth pressure increments of underground retaining wall under different H/w

excavation depth to excavation distance (H/s=2.67, 4, 8) with the same lateral width w and excavation width B are compared. The two selected test groups corresponding to the two conditions are tests 1, 2 and 3 (w=600 mm, B=75 mm) and tests 4, 5, and 6 (w=600 mm, B=150 mm), respectively. The relationships between the earth pressure increments of the retaining wall and the normalized burial depth are shown in Fig. 7.

For Series S in Fig. 7, under the same ground loss rate, the upper part of the earth pressure increments on the retaining wall of test S3 (H/s=8) increase much larger than that in tests S1 and S2 with H/s=4 and 2.67. It indicates that the farther the excavation distance is, the smaller the influence of the underground excavation on the earth pressure of the retaining wall is. When H/s reaches 2.67, the influence of excavation on the earth pressure on the upper retaining wall is almost negligible.

For Series T in Fig. 7, the earth pressure increments are significantly larger than that observed in Series S. With the increase of H/s, the earth pressure increments decreases a little. The influence of the excavation distance on the earth pressure of the retaining structure is relatively small.

4.6 The influence of the ratio of tunnel excavation depth to lateral width

For different tunnel excavation depth to lateral width ratios (H/w=1, 1.3, and 2), the test groups with the same

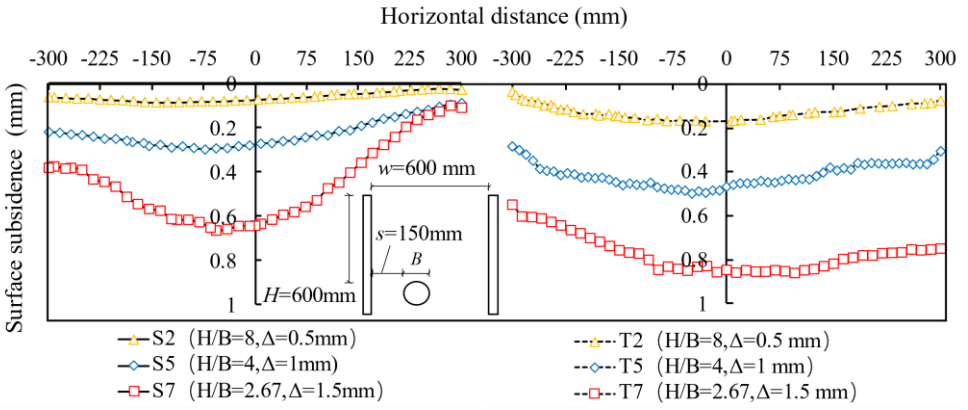

(a) w=600 mm, s=150 mm

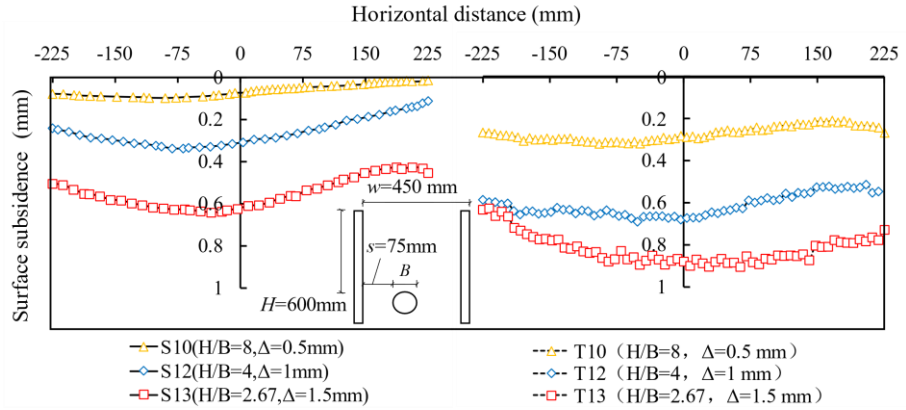

(b) w=450 mm, s=75 mm

Fig. 9 Ground settlement curves for different *H*/*B*

excavation distance *s* and excavation width *B* are selected for each condition. The test groups consist of tests 3, 10, and 14 (*s*=75 mm, *B*=75 mm), and tests 6, 12, and 15 (*s*=75 mm, *B*=150 mm), respectively. The relationships between the earth pressure increments of the retaining wall and the normalized burial depth *z*/*H* are shown in Fig. 8.

For Series S in Fig. 8, under the same ground loss rate, with the increase of *H*/*w*, the range of the earth pressure reduction at the bottom of the retaining wall increase a little, but the earth pressure above the turning point weakens. This indicates that the excavation in the narrow space is likely to cause reduction of the earth pressure on the retaining structure.

For Series T in Fig. 8, under the same ground loss rate, the earth pressure increments are larger than those in Series S, and the earth pressure on the lower part of the retaining structure has larger increments. With the increase of *H*/*w*, the earth pressure increments decrease gradually. At *H*/*w* =2, the earth pressure increments on the upper part of retaining structure is rather small.

5. The influence of under-crossing tunneling on the ground settlement

5.1 The influence of the ratio of tunnel excavation depth to excavation width

To study the influence of *H*/*B* on the ground settlement curve when the tunnel passes through the adjacent existing and newly-built underground retaining structure, the test groups with the same lateral width *w* and excavation distance *s* are selected for each conditions with *H*/*B*=8, 4, and 2.7. The two test groups are composed of tests 2, 5, and 7 (*w*=600 mm, *s*=150 mm) and tests 10, 12, and 13 (*w*=450 mm, *s*=75 mm), respectively. The ground settlement curves of the two test groups are shown in Fig. 9.

As is shown in Fig. 9, with the decrease of *H*/*B*, the curvature of the curve becomes larger and the curve turns steeper. For the same burial depth *H*, larger excavation width *B* means greater ground loss, which causes the increase of maximum ground settlement.

For Series T, the curvature of the curves and the maximum ground settlements are smaller and greater than those of Series S due to influence of the displacement of the retaining structure compared to those of Series S with the retaining structure at rest. With the decrease of *H*/*B*, the maximum ground settlement increases.

5.2 The influence of the ratio of tunnel excavation depth to excavation distance

For different ratios of tunnel excavation depth to excavation distance (*H*/*s*=2.67, 4, and 8), the test groups with the same lateral width *w* and excavation width *B* are

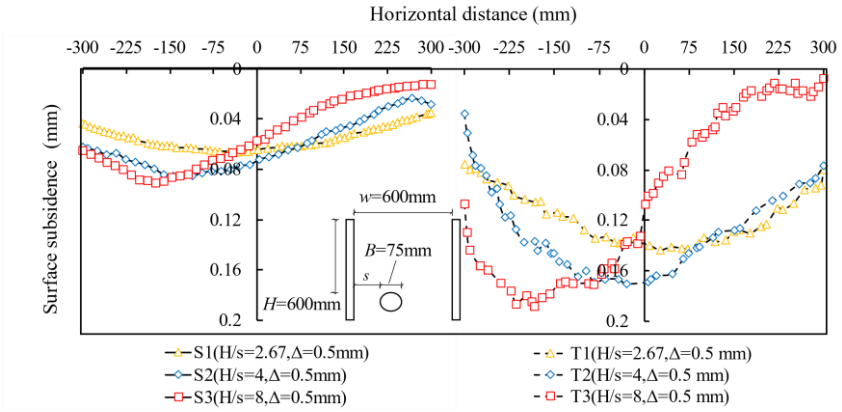

(a) w=600 mm, B=75 mm

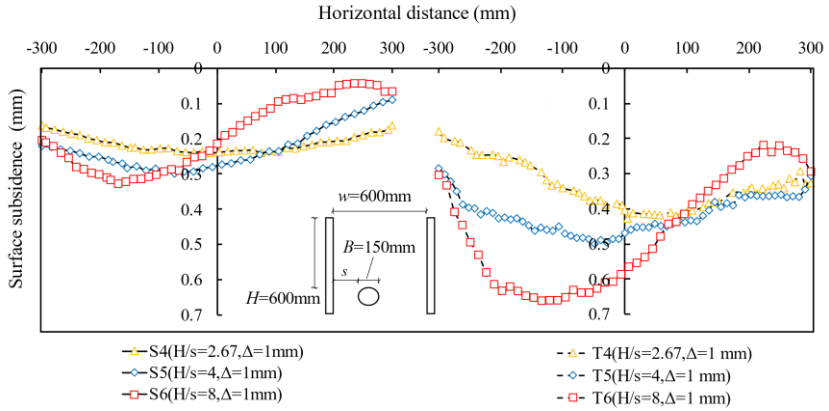

(b) w=600 mm, B=150 mm

Fig. 10 Ground settlement curves for different *H*/*s*

selected for each condition. The two test groups consist of tests 1, 2, and 3 (*w*=600 mm, *B*=75 mm) and tests 4, 5, and 6 (*w*=600 mm, *B*=150 mm), respectively. The ground settlement curves of the two test groups are shown in Fig. 10.

For Series S in Fig. 10, with the increase of the ratio of tunnel excavation depth to excavation distance *H*/*s*, the maximum ground settlement and the curvature of the ground settlement curve gradually increase. In terms of asymmetric excavation, smaller excavation distance means greater extent of asymmetric excavation, which causes the above trend of ground settlement curve.

For Series T in Fig. 10, compared to Series S with the retaining wall at rest, the shape of the ground settlement curve is similar, but the maximum ground settlement is larger and the curvatures on the right-side are smaller. When *H*/*s* is smaller, the curve is relatively flatter and the curvature is smaller. With the increases of the ratio of tunnel excavation depth, the maximum ground settlement and the curvature of the ground settlement curve increase.

5.3 The influence of the ratio of tunnel excavation depth to lateral width

Tests 3, 10, and 14 (*s*=75 mm, *B*=75 mm) and tests 6, 12, and 15 (*w*=75 mm, *B*=15 0 mm) with different ratios of tunnel excavation depth to lateral width (*H*/*w*=1, 1.3, and 2) form two test groups with the same excavation distance *s* and excavation width *B*. The ground settlement curves of each group are shown in Fig. 11.

For Series S in Fig. 11, the maximum ground settlement and the curvature of the ground settlement curve are largest when *H*/*w*=2. The maximum ground settlement decrease with the decrease of *H*/*w*.

For Series T in Fig. 11, compared with Series S with the retaining wall at rest, the shapes of the ground settlement curves at *H*/*w* =1 are similar "spoon" shape. The maximum ground settlement is larger than that of Series S with the retaining wall at rest. With the increase of *H*/*w*, the maximum ground settlement increases gradually. However, the curvature of the ground settlement curve decreases and the curves tend to be flat, which is opposite to that of Series S.

6. Conclusions

This paper presents an experimental analysis of earth pressure on retaining wall and ground settlement subjected to under-crossing of a tunnel using a two-dimensional test setup and an analogical soil. The ground loss induced by tunnel excavation was simulated by the settlement of a trapdoor and the active limit state of the retaining structure is modelled by the translation movement of the retaining

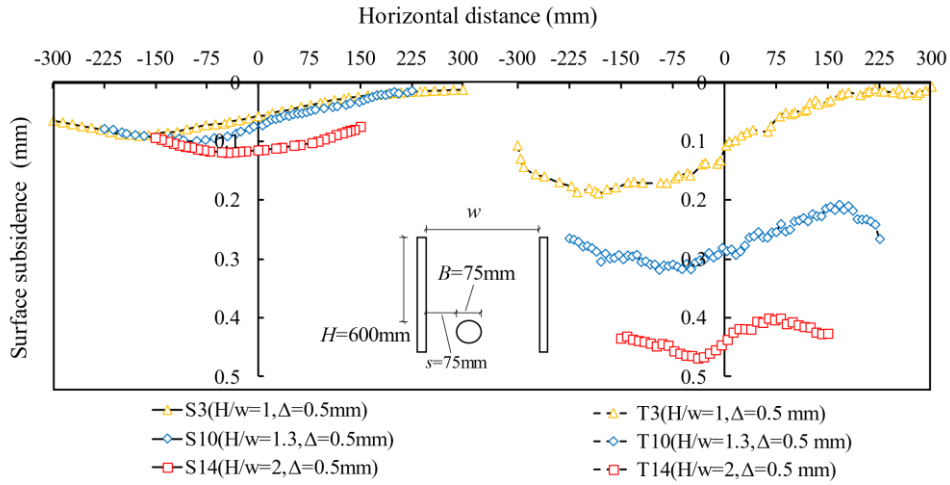

(a) s=75 mm, B=75 mm

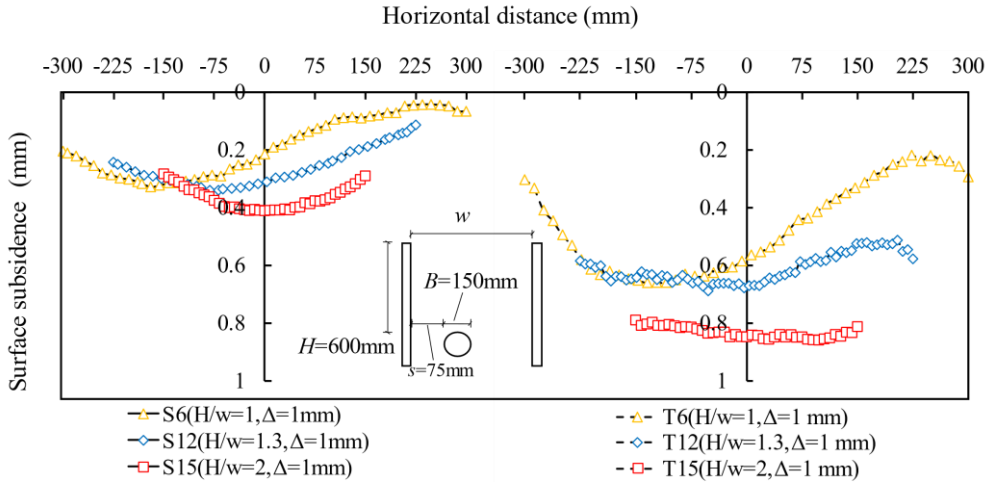

(b) s=75 mm, B=150 mm

Fig. 11 Ground settlement curves for different *H*/*w*

plate. Two conditions are considered which are tunnel crossing adjacent (1) existing and (2) newly-built underground retaining structures. Through 15 model tests for each condition, the influencing factors such as the lateral width, the excavation distance, and the excavation width are taken into account. The main conclusions can be drawn as follows:

- Under the condition of lateral confinement, the static earth pressure of retaining wall is between the calculation of the Jaky's method and the Janssen's method. When the lateral width is small, the earth pressure at rest exhibits a nonlinear distribution, which is close to the calculation result of Janssen's method. The retaining wall reaches the active limit state when the active displacement reaches 0.4%*H*. The active earth pressure exhibits a nonlinear distribution, which agrees best with the calculation result of the Paik's method.
- For the TCE condition, the earth pressure at the bottom of the retaining wall decreases with the setlement of the trapdoor, while the earth pressure at the upper part increases. For the TCN condition, the backfill is disturbed, the earth pressure increments of the retaining wall increases all the way. With the settlement of the trapdoor, the earth pressure increments of the retaining wall becomes larger.
- For the TCE condition, the ground loss causes the decrease of the earth pressure at the bottom of the retaining structure, while the earth pressure above a certain burial depth increases due to the arching effect. With the decrease of *H*/*B*, the earth pressure increments, maximum ground settlement and the curvature of the ground settlement decrease. These quantities are negatively related to *H*/*B* and positively related to *H*/*s* and *H*/*w*.
- For the TCN condition, the earth pressure increments referring to the active earth pressure on the underground retaining structure are all positive. Under the same parameters, the maximum ground settlement is larger than that observed in TCE condition. The maximum ground settlement and the curvature of the ground settlement are positively related to *H*/*s* while the earth pressure is subtly affected by *H*/*s*. With the increase of

H/*w*, the maximum ground settlement increase, but the earth pressure increments and the curvature of ground settlement decrease.

This paper makes relatively idealized assumptions for the excavation of the tunnel crossing adjacent underground retaining wall within shallow depth below the ground level. For example, the tunnel excavation is simplified as trapdoor settlement, and the displacement of the newly-built retaining wall is simulated by the translation of retaining plate. There are certain differences between these assumptions and the actual situation. Because the adopted analogous soil made of steel rod is cohesionless, this paper cannot consider more complicated working condition such as excavation under cohesive soil or rock. It is also quite difficult to fully reproduce the in-situ soil stress condition by using analogical soil in model test. Therefore, the analyses in all cases in this paper only provide a qualitative regularity and assessment for the tunnel construction safety under confined space conditions.

Acknowledgments

The research described in this paper was financially supported by the National Natural Science Foundation of China (No. 51909192).

References

Attewell, P.B. and Woodman, J.P. (1982), "Predicting the dynamics of ground settlement and its derivatives caused by tunneling in soil", *Ground Eng.*, **15**(8), 13-20.

Buchatskii, G.V., Zaitsev, A.N., Chernyakov, E.V., Bartoshevich, I.K., Konovalov, P.A. and Nikiforova, N.S. (2001), "Experience with construction of underground sections of buildings by the 'From top down' scheme", *Soil Mech. Found. Eng.*, **38**(4), 137-141. https://doi.org/10.1023/A:1012512125133.

Chakeri, H., Ozcelik, Y. and Unver, B. (2013), "Effects of important factors on surface settlement prediction for metro tunnel excavated by EPB", *Tunn. Undergr. Sp.Tech.*, **36**, 14-23. https://doi.org/10.1016/j.tust.2013.02.002.

Coulomb, C.A. (1776), "Essais sur une application des regles des maximis et minimis a quelques problems de statique relatits a l'architecture", Mem. Acad. Roy. Pres. Divers, Sav., Paris, France.

Dias, D. and Kastner, R. (2013), "Movements caused by the excavation of tunnels using face pressurized shields —Analysis of monitoring and numerical modeling results", *Eng. Geol.*, **152**(1), 17-25. https://doi.org/10.1016/j.enggeo.2012.10.002.

Ding, Z., Wei, X.J. and Wei, G. (2017), "Prediction methods on tunnel-excavation induced surface settlement around adjacent building", *Geomech. Eng.*, **12**(2), 185-195. https://doi.org/10.12989/GAE.2017.12.2.185.

Handy, L.R. (1985), "The arch in soil arching", *J. Geotech. Eng. -ASCE*, **111**(3), 302-318. https://doi.org/10.1061/(ASCE)0733-9410(1985)111:3(302).

Harrop-Williams, K.O. (1989), "Geostatic wall pressures", *J. Geotech. Eng. -ASCE*, **115**(9), 1321-1325. https://doi.org/10.1061/(ASCE)0733-9410(1989)115:9(1321).

Hesami, S., Ahmadi, S. and Ghalesari A.T. (2019), "Ground surface settlement prediction in urban areas due to tunnel excavation by the NATM", *Elec. J. Geotech. Eng.*, **18**, 1961-1972.

Hunt, D.V.L., Makana, L.O., Jefferson, I. and Rogers, C.D.F. (2016), "Liveable cities and urban underground space", *Tunn. Undergr. Sp. Tech.*, **55**, 8-20. https://doi.org/10.1016/j.tust.2015.11.015.

Jaky, J. (1944), "The coefficient of earth pressure at rest", *J. Soc. Hungarian Archit. Engineers*, **78**(22), 355-358.

Janssen, H.A. (1895), "Versuche uber Getreidedruck in Silozellen", *Verein Deutscher Ingenieure*, **39**, 1045-1049. (Partial English Translation in Proceedings of Institute of Civil Engineers, London, England, 1896: 553.)

Jenck, O. and Dias, D. (2004), "3D-finite difference analysis of the interaction between concrete building and shallow tunnelling", *Géotechnique*, **54**(8), 519-528. https://doi.org/10.1680/geot.2004.54.8.519.

Kakrasul, J.I. (2018), "Geosynthetic-reinforced retaining walls with limited fill space under static footing loading", Ph.D. Dissertation, Department of Civil, Environmental, and Architectural Engineering, University of Kansas, Lawrence.

Kavvadas, M.J. (2005), "Monitoring ground deformation in tunnelling: Current practice in transportation tunnels", *Eng. Geol.*, **79**(1-2), 93-113. https://doi.org/10.1016/j.enggeo.2004.10.011.

Khosravi, M.H., Pipatpongsa, T. and Takemura, J. (2013), "Experimental analysis of earth pressure against rigid retaining walls under translation mode", *Géotechnique*, **63**(12), 1020. https://doi.org/10.1680/geot.12.P.021.

Lam, S.Y., Haigh, S.K. and Bolton, M.D. (2014), "Understanding ground deformation mechanisms for multi-propped excavation in soft clay", *Soils Found.*, **54**(3), 296-312. https://doi.org/10.1016/j.sandf.2014.04.005.

Lee, S.W. (2019), "Experimental study on effect of underground excavation distance on the behavior of retaining wall", *Geomech. Eng.*, **17**(5), 413-420. https://doi.org/10.12989/gae.2019.17.5.413.

Leung, C. and Meguid, M.A. (2011), "An experimental study of the effect of local contact loss on the earth pressure distribution on existing tunnel linings", *Tunn. Undergr. Sp. Tech.*, **26**(1), 139-145. https://doi.org/10.1016/j.tust.2010.08.003.

Matsuo, M., Kenmochi, S. and Yagi, H. (1978), "Experimental study on earth pressure of retaining wall by field tests", *J. Jap. Soc. Soil Mech. Found. Eng.*, **18**(3), 27-41. https://doi.org/10.3208/sandf1972.18.3_27.

Paik, K.H. and Salgado, R. (2003), "Estimation of active earth pressure against rigid retaining walls considering arching effects", *Géotechnique*, **53**(7), 643-654. https://doi.org/10.1680/geot.2003.53.7.643.

Peck, R.B. (1969), "Deep excavations and tunneling in soft ground", *Proceedings of the 7th International Conference of Soil Mechanics & Foundation Engineering*, Mexico.

Rankine, W.J.M. (1857), "On the stability of loose earth", *Philos. T. Roy. Soc. London*, **147**, 9-27.

Rowe, R.K., Lo, K.Y. and Kack, G.J. (1983), "A method of estimating surface settlement above tunnels constructed in soft ground", *Can. Geotech. J.*, **20**(1), 11-22. https://doi.org/10.1139/t83-002.

Rui, R., Zhai, Y.X., Han, J., van Eekelen, S.J.M. and Chen, C. (2019), "Deformations in trapdoor tests and piled embankments", *Geosynthetics Int.*, **27**(2), 219-235. https://doi.org/10.1680/jgein.19.00014.

Som, M.N. and Das, S.C. (2003), Theory and Practice of Foundation Design, PHI Learning Pvt. Ltd., Delhi, India.

Srikar, G. and Mittal, S. (2021), "Analysis of retaining wall built near rock face for different wall movements", *Indian Geotech. J.*, 1-10. https://doi.org/10.1007/s40098-021-00548-1.

Stiros, S.C. and Kontogianni, V.A. (2009), "Coulomb stress changes: from earthquakes to underground excavation failures", *Int. J. Rock Mech. Min. Sci.*, **46**(1), 182-187.

https://doi.org/10.1016/j.ijrmms.2008.09.013.
Terzaghi, K. (1934), "Large retaining wall test", *Eng. News Record*, **112**(20), 136-140.
Wei, G. (2010), "Selection and distribution of ground loss ratio induced by shield tunnel construction", *Chinese J. Geotech. Eng*., **32**(9), 1354-1361.
White, D.J., Take, W.A. and Bolton, M.D. (2003), "Soil deformation measurement using particle image velocimetry (PIV) and photogrammetry", *Géotechnique*, **53**(7), 619-631. https://doi.org/10.1680/geot.2003.53.7.619.
Yamaguchi, I., Yamazaki, I. and Kiritani, Y. (1998), "Study of ground-tunnel interactions of four shield tunnels drive in close proximity, in relation to design and construction of parallel tunnels", *Tunn. Undergr. Sp. Tech.*, **13**(3), 289-304. https://doi.org/10.1016/S0886-7798(98)00063-7.
Yoo, C., Park, S.W., Kim, B. and Ban, H. (2019), Geotechnical aspects of underground construction in soft ground. CRC Press, Boca Raton, FL, USA.
Yum, S.G., Ahn, S., Bae, J. and Kim, J.M. (2020), "Assessing the risk of natural disaster-induced losses to tunnel-construction projects using empirical financial-loss data from South Korea", *Sustainability*, **12**(19), 8026. https://doi.org/10.3390/su12198026.

JS